DYNAMIC STIFFNESS FOR VIBRATION ANALYSIS OF LARGE MACHINE FOUNDATIONS ON SOFT SOILS STABILIZED BY DEEP MIXING

M. Tabatabaie[1], L. Mejia[2], S. C. Wu[3], M. Galagoda[4]
[1,2] URS Corp., Oakland, California, U.S.A.
[3,4] Bechtel Corp., Houston, Texas, U.S.A.

Abstract -- **This paper presents the results of soil structure interaction analyses using the computer program SASSI to develop foundation dynamic stiffness parameters for a 50-m-by-50-m mat foundation supporting vibrating machinery having operating frequencies of 60-80 Hertz. The soil profile consists of a thick layer of soft and loose recent marine sediments stabilized by deep soil mixing, underlain by very stiff clayey soils.**

To simplify the analytical model, the soil-cement columns and weak soil layers were replaced with an equivalent soil profile of calibrated engineering properties that resulted in the same foundation response as the actual system at frequencies less than 4 Hertz. This low-frequency calibrated profile was then used with a refined finite element model of the mat to analyze the foundation dynamic stiffness at frequencies of 60-80 Hertz

Two cases corresponding to rigid and flexible mats are analyzed. For the rigid mat, the foundation dynamic stiffness parameters are presented in terms of horizontal, vertical and rocking components at the center of the mat. For the flexible mat, these properties are presented in terms of mid-estimate with upper and lower bound values that account for the mat flexibility. Finally, comparisons of the rigid and flexible mat stiffness properties are presented.

Keywords -- **Deep soil mixing, dynamic stiffness, machine foundation, Soil structure interaction, vibration**

INTRODUCTION

An industrial facility in Trinidad required dynamic design of 50-m-by-50-m mat foundation to support vibrating machinery having operating frequencies of 60-80 Hertz. The foundations are designed for maximum dynamic displacements of less than 0.2 mils. The soil profile consists of a thick layer of soft and loose recent marine sediments (RMS) underlain by very stiff clayey soils. Deep soil mixing (DSM) was used to stabilize the soft/loose foundation soils with overlapping soil-cement columns that form a cellular grid system. The foundation mat rests on top of the grid columns at ground surface.

The large size of the mats and high frequency vibration response preclude the use of published design charts and simplified methods for evaluating foundation dynamic stiffness [1, 2, 3, 4 and 5]. In addition, the presence of soil-cement columns under the mats present significant modeling challenges, especially at high frequencies. To overcome these difficulties, a calibration study was undertaken to develop an equivalent horizontally layered system to represent the treated foundation media. The computer program SASSI [6, 7 and 8] was used to analyze the soil-structure interaction (SSI) problem. To make the model manageable in terms of computer processing and storage, the calibration analyses were performed on a relatively coarse finite element model discretized to transmit vibration frequencies of up to 4 Hz. The calibrated layered system was then used with a finely discretized finite element model of the mat foundation to analyze the foundation dynamic stiffness at frequencies of 60-80 Hz.

The methodology used to develop the foundation dynamic stiffness parameters for the rigid and flexible mats considered in the present study are discussed in detail in Appendix A. The foundation calibration analyses to develop an equivalent horizontally layered system to represent the treated foundation are discussed first. Following this the results of the foundation dynamic stiffness for selected vibration modes of the rigid and flexible mats are presented. Finally, the dynamic stiffness of the rigid and flexible mats are compared to gain insight into the effects of the assumed mat stiffness so that conclusions can be drawn with respect to the applicability of rigid mat solutions to an otherwise flexible mat

FOUNDATION CALIBRATION STUDY

The large size of the mats and the presence of the soil-cement columns under the mats presented significant challenges in developing an appropriate three-dimensional analytical model, especially at high frequencies. The size of the required mesh to accurately represent the physical characteristics of the treated zone would require an extremely large finite element mesh, and would make the computations impossible to handle with available computers. Therefore, to simplify the analytical model for the foundation system, the soil-cement columns and the RMS layer were replaced with an equivalent uniform layer with appropriate engineering characteristics that would result in the same foundation response as the actual foundation. The following describes the study undertaken to develop this equivalent soil profile (ESP) to replace the DSM-stabilized foundation, to facilitate the numerical analyses.

A. DSM-Stabilized Soil Profile and Properties

The actual DSM-stabilized soil profile is shown in Fig. 2(a). It consists of an 8.5-m-thick layer of relatively soft and weak sediments (RMS) underlain by very stiff to hard clayey soils (OMS). The top 3.5 m of the OMS is weathered. The groundwater is at 1.5 m below the ground surface. Deep soil mixing has been used to treat the soft foundation soils (primarily the RMS layer) to allow support of the facilities on mat foundations. The foundation treatment consisted of installing soil-cement columns to a depth of approximately 12 m below the ground surface (to the bottom of the weathered OMS layer). The soil-cement columns were constructed with an overlap to form a wall with an effective width of about 0.828 m. The soil-cement walls were laid out in a grid pattern with uniform spacing of about 4.5 m center-to-center (c/c). Table 1 lists the foundation soil and soil-cement wall material properties.

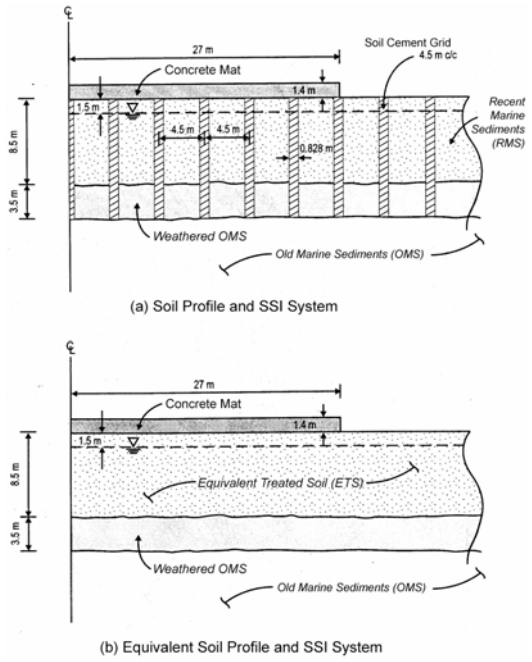

Fig. 2: Idealized Soil Profiles for Calibration Study

TABLE 1: MATERIAL PROPERTIES OF FOUNDATION SOILS

Elastic Properties	Native Soils				
	RMS Above Water Table	RMS Below Water Table	Weathered OMS	OMS	Soil-Cement Wall
Shear Modulus (MPa), G	34	34	160	350	450
Young's Modulus (MPa), E	91.8	100.6	473.6	1,036	1,035
Poisson's Ratio, ν	0.35	0.48	0.48	0.48	0.15
Density (kg/m^3), ρ	1,630	1,630	1,845	2,000	1,940

B. Calibrated Equivalent Soil Profile and Properties

The equivalent soil profile is shown in Fig. 2(b). This profile is the same as the actual DSM-stabilized soil profile shown in Fig. 2(a) except that the soil-cement columns and the RMS layer are replaced by an equivalent treated soil (ETS). To calibrate the properties of the ETS layer, four low-frequency SASSI models were developed and analyzed to determine the foundation dynamic stiffness. The characteristics of these models are summarized in Table 3.

TABLE 3: SASSI CALIBRATION MODELS

Property	Model			
	SC-0	SC-3	SC-5	SC-N
Mat Size	54-m Square	54-m Square	54-m Square	54-m Square
Profile	Actual	Actual	Actual	ESP
No. of Soil-Cement Columns Below Mat	13	13	13	0
No. of Soil-Cement Columns Beyond Mat	0	3	5	0

The models used a 54-m rigid massless square mat at the ground surface. The first three models (SC-0, SC-3 and SC-5) used the actual DSM-stabilized soil profile, as shown in Fig. 2(a). They included 13 soil-cement cells at 4.5 m c/c below the mat, and 0, 3 and 5 soil-cement cells, respectively, beyond the edge of the mat on all four sides. The fourth model (SC-N) is supported at the surface of the equivalent soil profile, as shown in Fig. 2(b). Because no soil-cement grid system is included, the number of interaction nodes is significantly reduced.

The finite element model for one of these models is shown in Fig. 3. Because of the geometrical symmetry, only ¼ of the model was analyzed. The mat consists of 36 flat shell elements. The soil-cement grid walls were modeled with 1,056 flat shell elements connected to the mat nodes at the top. The soil elements within the grid cells were modeled using 484 8-node solid elements connected to the soil-cement shell nodes. The soil profile outside the treated zone consisted of a horizontally layered soil system over a uniform halfspace.

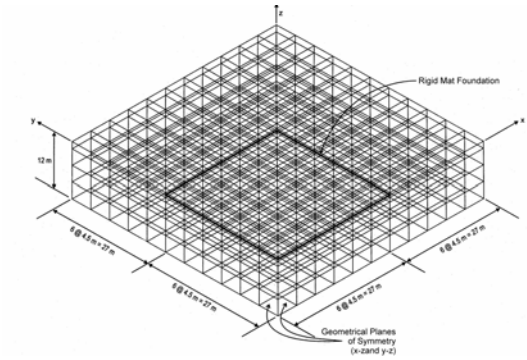

Fig. 3: Finite Element SASSI Model SC-5

The computed vertical, horizontal, and rocking foundation stiffness for zero frequency (static) for the first three models is compared in Table 3. In addition, the foundation stiffness versus the number of soil-cement rows beyond the edge of the mat is plotted in Fig. 4 for the horizontal component (the same results are observed for the vertical and rocking components). These results indicate that as the number of soil-cement rows increases beyond the edge of the mat (or in other words, as the treated soil zone extends farther beyond the mat area), the foundation stiffness becomes larger, as expected for all three modes of loading. However, after approximately 5 soil-cement rows beyond the edge of the mat, the foundation stiffness for all three modes of vibration is no longer affected significantly by the number of soil-cement rows beyond the edge of the mat.

Therefore, using Model SC-5 as the target model for calibration, SASSI analyses of Model SC-N were performed using different ETS properties to match the results of Model SC-5 in terms of vertical, horizontal, and rocking foundation stiffness. Based on these analyses, the final calibrated properties of the ETS were G = 135 MPa, ν = 0.48, and ρ = 1,630 kg/m^3. Table 3 presents a comparison of the computed foundation static stiffness. As seen from Table 3 the SC-N model using the above calibrated ESP properties results in foundation static stiffness values that are within 1 to 3 percent of those of Model SC-5 for all three modes of vibration.

TABLE 3: COMPARISON OF FOUNDATION STATIC STIFFNESS, CALIBRATION STUDY

Model	K_x (MN/m)	K_z (MN/m)	K_{yy} (MN-m/Rad)
SC-0	26,970	68,995	33,376,724
SC-3	30,855	72,888	38,091,023
SC-5	31,573	72,993	38,162,981
SC-N	31,985	73,933	37,102,617

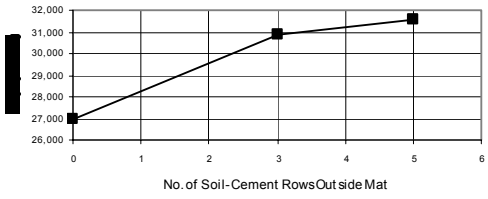

Fig. 4: Foundation Static Stiffness, Calibration Study

In addition to the foundation static stiffness, the shape of the foundation dynamic stiffness (in terms of stiffness and damping coefficients) for Models SC-0, SC-3 and SC-5 was also compared as a function of frequency of vibration to that of Model SC-N using calibrated ESP properties. Comparisons of the results for the horizontal, component are presented in Figures 5 (the same trends are also observed for the vertical and rocking components). These results also indicate that as the soil-cement treated zone extends farther beyond the edge of the mat, the normalized foundation dynamic stiffness curves converge to, and show reasonable agreement with, those of the calibrated Model SC-N.

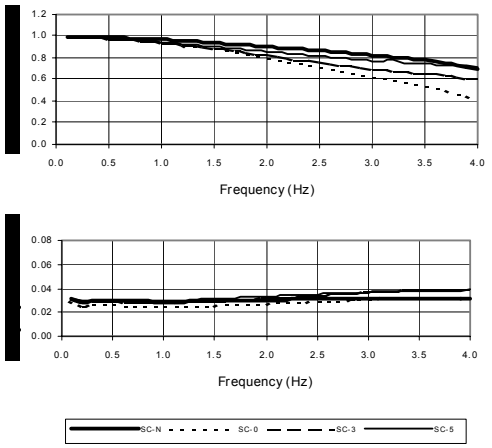

Fig. 5: Comparison of Foundation Dynamic Stiffness Coefficients, Calibration Study, Horizontal (x) Component

FOUNDATION DYNAMIC STIFFNESS ANALYSES

The calibrated equivalent soil profile developed above was used to evaluate the foundation dynamic stiffness parameters for the mat foundation subjected to vibration frequencies of 60-80 Hz. To allow proper numerical modeling of high frequency vibrations, a finely discretized finite element model of the mat foundation was developed to satisfy the criteria for transmission of wavelengths corresponding to f_{max} = 80 Hz. This model is shown in Fig. 6.

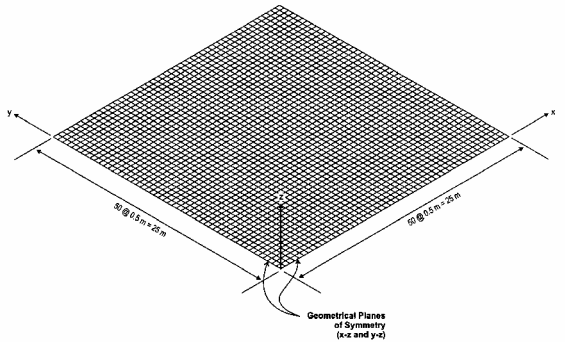

Fig. 6: Finite Element SASSI Model, 50-m-by-50-m Mat

A. Rigid Mat Foundation

In this case, the mat is assumed to be massless and behave rigidly. The foundation dynamic stiffness amplitudes versus frequency of vibration for the horizontal x, vertical z, and rocking yy components are shown in Figures 7, 8 and 9, respectively. These results cover the frequency range of 60 to 80 Hz.

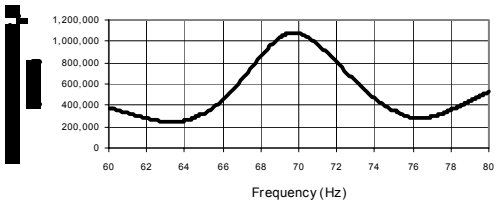

Fig. 7: Foundation Dynamic Stiffness Amplitude, Rigid Mat, Horizontal (x) Component

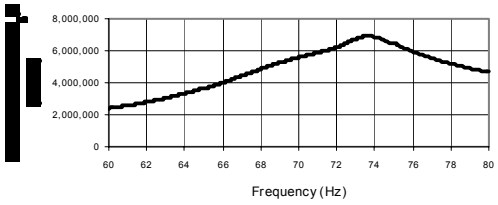

Fig. 8: Foundation Dynamic Stiffness Amplitude, Rigid Mat, Vertical (z) Component

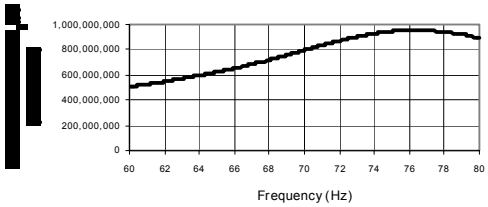

Fig. 9: Foundation Dynamic Stiffness Amplitude, Rigid Mat, Rocking (yy) Component

B. Flexible Mat Foundation

The 50-m-by-50-m flexible mat foundation was analyzed using SASSI in much the same way that the rigid mat was analyzed, except that the elastic properties of a concrete mat as listed below were used in the analyses. It is noted that for these calculations, the mat is assumed to be massless.

Mat thickness = 1.4 m
Concrete compressive strength = 27,580 KPa
Young's modulus = 24,855 MPa
Poisson's Ratio = 0.17
Mass Density = 0.

As discussed above, presentation of the foundation dynamic stiffness properties for a flexible mat is not simple because the overall behavior of the mat cannot be described by six degrees of freedom (three translations and three rotations). Therefore, it is desirable to provide the response of the mat for more than one point. The preferred locations are the center of the mat, the corners, and the mid-points along the sides of the mat, as shown in Fig. 15. In this way, it is possible to better account for the effects of the mat deformations on the dynamic response of the structure.

The subgrade dynamic stiffness properties of the flexible, massless mat were developed at the center (Point 1), corners (Point 3) and mid-points along the mat sides (Points 2 and 4). The results in terms of subgrade dynamic stiffness per unit area of the mat are presented in Figures 16 and 17 for the horizontal x, and vertical z components, respectively.

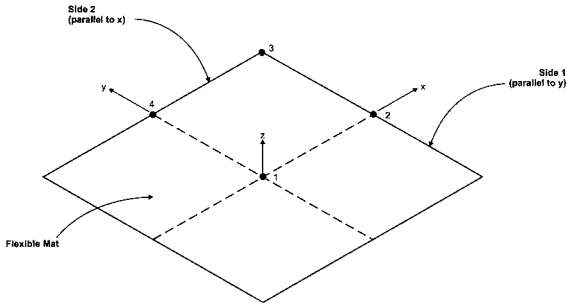

Fig. 15: Subgrade Stiffness Locations

As an alternative representation of the flexible mat foundation stiffness, the global subgrade dynamic stiffness of the flexible mat was calculated following the procedure outlined above. The results are shown in Figures 18, 19 and 20 for the horizontal x, vertical z and rocking yy components, respectively. The results for the vertical and rocking modes incorporate a range of stiffness properties (upper and lower bound) based on the vertical subgrade stiffness calculated at the center, corners and mid-points along the mat sides to reflect the effects of the mat flexibility, as discussed below. No range was necessary for the horizontal stiffness, as the mat was found to behave fairly rigid in this mode.

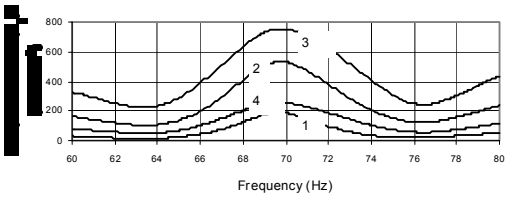

Fig. 10: Subgrade Dynamic Stiffness Per Unit Area, Flexible Mat, Horizontal (x) Component

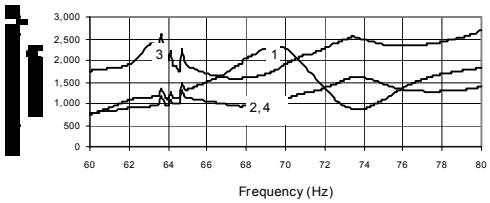

Fig. 11: Subgrade Dynamic Stiffness Per Unit Area Flexible Mat, Vertical (z) Component

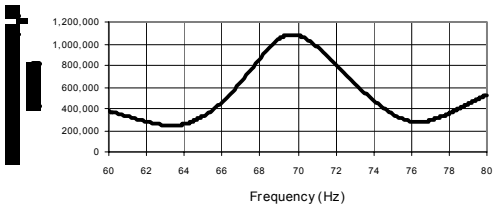

Fig. 12: Global Subgrade Dynamic Stiffness Amplitude, Flexible Mat, Horizontal (x) Component

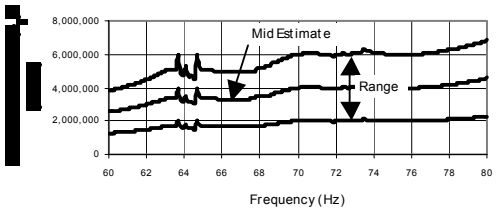

Fig. 13: Global Subgrade Dynamic Stiffness Amplitude, Flexible Mat, Vertical (z) Component

COMPARISON OF RIGID AND FLEXIBLE MAT STIFFNESS

The subgrade dynamic stiffness of the rigid and flexible mats were compared to gain insight into the effects of the assumed mat stiffness so that conclusions can be drawn with respect to the applicability of rigid mat solutions to an otherwise flexible mat. Following the same procedure that was used for flexible mats, the subgrade stiffness properties for the 50-m-by-50-m rigid mat were computed at the center, corners and mid-points along the mat sides. The results are shown in Figures 21 and 22 for the horizontal x and vertical z components, respectively.

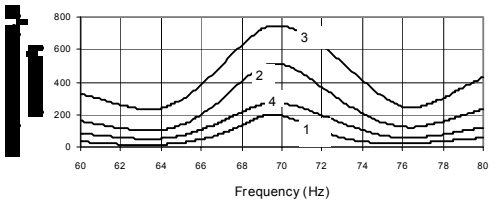

Fig. 14: Subgrade Dynamic Stiffness, Rigid Mat, Horizontal (x) Component

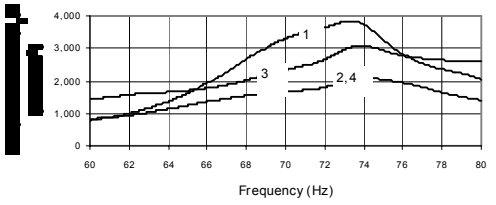

Fig. 15: Subgrade Dynamic Stiffness, Rigid Mat, Vertical (z) Component

Examination of the subgrade stiffness properties for the rigid and flexible mats (see Figures 16 through 17 for flexible and 21 and 22 for rigid mat) indicate that:

- In the horizontal (x and y) direction, the flexible mat behaves as if it was nearly rigid. The subgrade dynamic stiffness of the rigid and flexible mats computed at the center, corners and mid-points along the mat sides are approximately the same. Similarly, the global subgrade stiffness computed at the center of the flexible mat (Fig. 18) is very similar to the foundation stiffness of the rigid mat (Fig. 12).
- In the vertical (z) direction, the flexible mat behavior is very different from that of the rigid mat, as shown by the computed subgrade dynamic stiffness properties at the center, corners and mid-points along the sides of the flexible and rigid mats. In addition the global subgrade stiffness of the flexible mat (Fig. 19) shows very different results from those of the rigid mat (Fig. 13)
- For rocking components, no direct comparison of the subgrade stiffness properties of the rigid and flexible mats were performed. However, a comparison of the foundation dynamic rocking stiffness of the rigid and flexible mats (see Fig. 20 for flexible and 14 for rigid mats) indicates similar behavior as for the vertical component.

SUMMARY AND CONCLUSIONS

Three-dimensional soil structure interaction analyses were performed using SASSI to develop foundation dynamic stiffness properties for a 50-m-by-50-m mat foundation supporting vibrating machinery having operating frequencies of 60-80 Hertz. The soil profile consists of a thick layer of soft and loose soil deposit underlain by very stiff clayey soils. Deep soil mixing was used to stabilize the weak foundation soils with overlapping soil-cement columns that form a cellular grid system. To simplify the analytical model, the soil-cement columns and weak soil layers were replaced with an equivalent soil profile of calibrated engineering properties that resulted in the same foundation response as the actual system at low frequencies. This profile was then used to develop the foundation dynamic stiffness at 60-80 Hertz. Two cases corresponding to a rigid and flexible mat stiffness were analyzed. For the rigid mat, the foundation dynamic stiffness coefficients and amplitudes were presented in terms of horizontal (x and y), vertical (z) and rocking (xx and yy) components at the center of the mat. For the flexible mat, the foundation stiffness were presented in terms of x and y components of the subgrade dynamic stiffness amplitudes computed at the center, corners and mid-points along the mat sides. In addition, mid-estimate global subgrade (foundation) dynamic stiffness components of the flexible mat were computed from the subgrade dynamic stiffness values

computed at all mat nodes. To account for the effects of mat flexibility, a range of stiffness properties (upper and lower bound) was estimated for the global subgrade stiffness based on the subgrade stiffness properties computed at the center, corners and mid-points along the mat sides. A comparison of the rigid and flexible mat results indicate that in the horizontal mode, the mat acts as if it was rigid but in the vertical and rocking modes its behavior is very different from that of the rigid mat.

REFERENCES

[1] F.E. Richart, J.R. Hall and R.D. Woods, "Vibrations of Soils and Foundations," Prentice-Hall, Englewood Cliffs, N.J., 1970.

[2] J.P. Wolf, Dynamic Soil Structure Interaction, Prentice Hall, 1985.

[3] J.P. Wolf, "Spring-Dashpot-Mass Models for Foundation Vibrations," Journal of Earthquake Engineering and Structural Dynamics, Vol. 26, 931-949, 1977.

[4] M. Preisig, and J.P. Wolf, "Dynamic Stiffness of Surface Foundation on Layered Halfspace Based on Wave Propagation in Cones," Presented at 5th European Conference on Numerical Methods in Geotechnical Engineering, Paris, September 2002.

[5] W. Whittaker and P. Christiano, "Dynamic Response of Plate on Elastic Halfspace," Journal of Engineering Mechanics Division, Vol. 108, No. EM1, 1982.

[6] J. Lysmer, M. Tabatabaie, F. Tajirian, S. Vahdani and F. Ostadan., "SASSI – A System for Analysis of Soil Structure Interaction," Report No. UCB/GT/81-02, Geotechnical Engineering, University of California, Berkeley, April 1981.

[7] M. Tabatabaie and F. Tajirian, "Vibration Analysis of Foundations on Layered Media," ASCE proceedings on Vibrations for Soils and Foundations, Detroit, Michigan, 1985.

[8] MTR/SASSI, "A System for Analysis of Soil Structure Interaction," Volume I, User's Manual and Volume II, Theoretical Manual, March 1998.

APPENDIX A

METHODOLOGY

Vibration analyses of machine foundations are generally performed in two steps. The foundation system is analyzed first to develop the foundation dynamic stiffness properties in terms of frequency-dependent stiffness and damping parameters. These parameters are then used at the base of the machine foundation model to analyze its dynamic response. For small amplitude vibrations, the soil strains are generally in the linear elastic range and the foundation dynamic stiffness parameters are not dependent on the amplitude of the load. These parameters are, however, influenced by the loading frequencies, the stiffness and geometry of the foundation and the soil layering and dynamic properties. Development of foundation dynamic stiffness for rigid and flexible mats is discussed below.

A. Rigid Mat Foundation

In general, the dynamic response of a rigid, massless, rectangular mat foundation supported at the ground surface and subject to harmonic force vibrations may be written as follows:

$$\underline{K}^* \cdot \underline{U}^* e^{i\omega t} = \underline{P}^* e^{i\omega t} \qquad (A.1)$$

Where:

$\underline{U}^*$ = 6 × 1 complex displacement vector
$\underline{P}^*$ = 6 × 1 complex load vector
$\underline{K}^*$ = 6 × 6 complex dynamic stiffness matrix
i = $\sqrt{-1}$
ω = 2 π f, circular frequency of vibration
t = time
f = frequency of vibration

In Eq. (A.1), the displacement and load vectors are referenced to the center of the mat (see Fig. A.1). For the special case of a square mat with two axes of symmetry (x and y), and excluding the rotation about the z-axis, the dynamic stiffness matrix, $\underline{K}^*$, is reduced to a 5 × 5 matrix with nine non-zero components, which include two horizontal ($K_x^* = K_y^*$), one vertical (K_z^*), two rocking ($K_{xx}^* = K_{yy}^*$), and four coupled horizontal-rocking ($K_{x\text{-}yy}^* = K_{yy\text{-}x}^* = -K_{y\text{-}xx}^* = -K_{xx\text{-}y}^*$). In this case, Eq. (A.1) may be written as follows:

$$\begin{vmatrix} K^*_x & 0 & 0 & 0 & K^*_{x\text{-}yy} \\ 0 & K^*_y & 0 & K^*_{y\text{-}xx} & 0 \\ 0 & 0 & K^*_z & 0 & 0 \\ 0 & K^*_{xx\text{-}y} & 0 & K^*_{xx} & 0 \\ K^*_{yy\text{-}x} & 0 & 0 & 0 & K^*_{yy} \end{vmatrix} \begin{vmatrix} U^*_x \\ U^*_y \\ U^*_z \\ \theta^*_{xx} \\ \theta^*_{yy} \end{vmatrix} = \begin{vmatrix} P^*_x \\ P^*_y \\ P^*_z \\ M^*_{xx} \\ M^*_{yy} \end{vmatrix} \qquad (A.2)$$

Where U and θ are displacements and rotations, respectively, and P and M are forces and moments, respectively, at the center of the mat. Equation (A.2) is used to represent the entire soil-rigid mat foundation system by the dynamic stiffness matrix, $\underline{K}^*$ for vibration analysis.

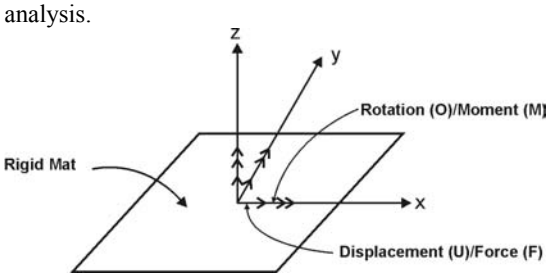

Fig. A.1: Mat Foundation Considered

In general, the dynamic stiffness matrix, $\underline{K}^*$, is complex and frequency-dependent. Each component of this matrix can be described in terms of a stiffness (spring) value and a damping (dashpot) value in accordance with Eq. (A.3).

$$K^* = K\,[k(\omega) + i\,\omega\,c(\omega)] \qquad (A.3)$$

Where:

K^* = Complex dynamic stiffness component
K = Static stiffness component
$k(\omega)$= Frequency-dependent stiffness coefficient
$c(\omega)$= Frequency-dependent damping coefficient

Thus, by specifying the static stiffness (K) and frequency-dependent stiffness and damping coefficients ($k(\omega)$ and $c(\omega)$) for each mode of vibration (horizontal, vertical, rocking and coupled horizontal-rocking), an equivalent spring-dashpot model can be developed to represent the foundation system.

For single harmonic foundation vibration analysis, the phasing information of the foundation dynamic stiffness may be conservatively ignored for computing the structural response. In this case, it is possible to provide the foundation dynamic stiffness in terms of its amplitude (K_o) calculated from Eq. (A.4). This greatly simplifies implementation of the foundation dynamic stiffness in the structural analyses.

$$K_o = K \cdot \sqrt{[k(\omega)^2 + \omega^2\, c(\omega)^2]} \qquad (A.4)$$

To develop the dynamic stiffness matrix for the rigid mat, a numerical finite element model of the mat was developed and analyzed using the computer program SASSI. Because of geometrical symmetry, only ¼ of the soil-mat foundation system was analyzed. Three load

cases corresponding to a unit amplitude uniformly distributed harmonic force in the x and z directions, and moment about the y-axis were analyzed to develop a 5×5 complex dynamic flexibility matrix ($\underline{F}^*$), which was then inverted to obtain the dynamic stiffness matrix ($\underline{K}^* = \underline{F}^{*-1}$), as shown in Eq. (A.5).

$$\underline{K}^* = \begin{vmatrix} F^*_x & 0 & 0 & 0 & F^*_{x\text{-}yy} \\ 0 & F^*_y & 0 & F^*_{y\text{-}xx} & 0 \\ 0 & 0 & F^*_z & 0 & 0 \\ 0 & F^*_{xx\text{-}y} & 0 & F^*_{xx} & 0 \\ F^*_{vy\text{-}x} & 0 & 0 & 0 & F^*_{yy} \end{vmatrix}^{-1} \quad \text{(A.5)}$$

The coupled horizontal-rocking stiffness components were also calculated, but since they are relatively small for these surface foundations, they are not presented herein.

B. Flexible Mat Foundation

The flexible mat foundation case is more complex than the rigid mat case described above. This is mainly due to the fact that the response of a flexible mat cannot be fully described by three translations and three rotations at the center of the mat. When the superstructure is connected to the flexible mat, each point on the mat moves differently, and it is not possible to develop one spring-dashpot model to represent the entire soil-flexible mat foundation system for each mode of vibration. A relatively large dynamic stiffness matrix incorporating many nodes on the mat is required to accurately represent the flexibility of the mat.

For the present study, we adopted a simplified approach to derive a set of subgrade dynamic stiffness properties at the center, corners, and mid-points along the mat sides. These stiffness properties, which are similar to soil springs attached to the bottom of the flexible mat are provided for two horizontal (x and y) and vertical (z) components. In this case, rotational soil springs are not defined and the overall rotational behavior of the mat is accommodated by the vertical dynamic soil springs.

To develop the subgrade dynamic stiffness properties, the mat foundation was analyzed for two load cases corresponding to uniformly distributed load with unit amplitude along the x- (or y-) and z-axes similar to those described above for the rigid mat. The corresponding displacements in the x (or y) and z directions, respectively, computed at various nodes on the mat were used to develop subgrade dynamic stiffness factors in accordance with Eq. (A.6).

$$k^*_{j,n} = q^*_{j,n} / U^*_{j,n} \quad \text{(A.6)}$$

Where :

$k^*_{j,n}$ = Complex subgrade stiffness (per unit area)
$q^*_{j,n} = r^*_{j,n} / A_n$, Complex contact stress below mat
$U^*_{j,n}$= Complex displacement of mat
$r^*_{j,n}$ = Complex soil reaction force below mat
A_n = Tributary area
j = x, y or z direction
n = Selected node on the mat (center, corner, et)

For the structural analyses of the flexible mat, the subgrade dynamic stiffness properties in x-, y- and z-directions at various points on the mat may be obtained by linear interpolation from those provided at the center, corners and mid-points along the mat sides.

Alternatively, to simplify the input for dynamic analysis of the structure, global subgrade dynamic stiffness for the entire mat foundation system was calculated by adding up the corresponding stiffness values obtained from Eq. (A.7) for translational (x, y and z) and Eq. (A.8) for rotational (xx and yy) components for all the mat nodes. For computation of the global rocking stiffness components, the mat was subjected to uniform harmonic moments of unit amplitude about the x and y axis.

$$K^*_j = SUM_{n=1,N}(r^*_{j,n} / U^*_{j,n}) \quad \text{(A.7)}$$

$$K^*_l = SUM_{n=1,N}(r^*_{j,n} \cdot L_n \cdot L_n \cdot / U^*_{j,n}) \quad \text{(A.8)}$$

Where:

K^*_j = Global subgrade dynamic stiffness
N = Number of nodes on the mat
n = Node number
L_n = Moment arm
l = xx or yy directions

The above global subgrade (foundation) dynamic stiffness parameters are representative of the average (mid estimate) stiffness for the entire flexible mat. To account for the effects of the mat flexibility, a range of stiffness properties (upper and lower bound) was estimated for the global subgrade stiffness based on the subgrade stiffness properties computed at the center, corners and mid-points along the mat sides. Although this is an approximate way of representing the flexible mat response, it is expected to bound the peak response within the upper and lower bound values.